

## Article

# Re-Austenitisation of Thin Ferrite Films in C–Mn Steels during Thermal Rebound at Continuously Cast Slab Corner Surfaces

Dannis Rorisang Nkarapa Maubane \*, Roelf Johannes Mostert  and Kevin Mark Banks

Department of Materials Science and Metallurgical Engineering, University of Pretoria, Pretoria 0002, South Africa

\* Correspondence: rorisang.maubane@up.ac.za

**Abstract:** The influence of primary cooling and rebound temperature at C–Mn slab corner surfaces during continuous casting on ferrite film transformation and AlN precipitation was investigated. Laboratory simulations included primary cooling to minimum temperature,  $T_{min}$ , rebounding to various maximum temperatures,  $T_{max}$ , followed by secondary cooling. The negative effect of a low  $T_{min}$  on hot ductility could not be readily reversed, even at relatively high temperatures. Quantitative metallography was employed to study the evolution of the microstructure during rebounding and secondary cooling. Following primary cooling to temperatures just above the  $Ar_3$ , thin films of allotriomorphic ferrite formed on the austenite grain boundaries. These films did not completely transform to austenite during the rebound at 3 °C/s up to temperatures as high as 1130 °C and persisted during slow secondary cooling up to the simulated straightening operation. Whilst dilatometry did not indicate the presence of ferrite after high rebound temperatures, metallography provided clear evidence of its existence, albeit in very small quantities. Coincident with the ferrite at these high temperatures was the predicted (TC-PRISMA) grain boundary precipitation of AlN in bcc iron during the rebound from a  $T_{min}$  of 730 °C. Importantly no thin ferrite films were observed, and AlN precipitation was not predicted to occur when  $T_{min}$  was restricted to 830 °C. Cooling below this temperature promotes austenite grain boundary ferrite films and AlN precipitation, which both increase the risk of corner cracking in C–Mn steels.

**Keywords:** continuous casting; primary cooling; rebound temperature; ferrite films; AlN



**Citation:** Maubane, D.R.N.; Mostert, R.J.; Banks, K.M. Re-Austenitisation of Thin Ferrite Films in C–Mn Steels during Thermal Rebound at Continuously Cast Slab Corner Surfaces. *Metals* **2022**, *12*, 2155. <https://doi.org/10.3390/met12122155>

Academic Editor: Barrie Mintz

Received: 9 November 2022

Accepted: 10 December 2022

Published: 15 December 2022

**Publisher's Note:** MDPI stays neutral with regard to jurisdictional claims in published maps and institutional affiliations.



**Copyright:** © 2022 by the authors. Licensee MDPI, Basel, Switzerland. This article is an open access article distributed under the terms and conditions of the Creative Commons Attribution (CC BY) license (<https://creativecommons.org/licenses/by/4.0/>).

## 1. Introduction

Transverse corner cracking (TCC) is a common problem experienced during the continuous casting of steel slabs. When the unbending/straightening process is performed at temperatures associated with low ductility, TCC can occur due to tensile strains induced at the top surface [1,2]. The causes of TCC in C–Mn steels include large as-cast austenite grain size (which encourages grain boundary crack propagation), the presence of thin ferrite films (strain concentration) and AlN particles (which promote crack formation by grain boundary sliding) on the austenite grain boundaries during unbending. In high-strength microalloyed steels, fine V, Nb, and Ti carbonitrides also contribute to lowering the hot ductility during unbending [2]. The chemical composition (precipitate formers) and process parameters, such as oscillation marks (pitch and depth), casting speed (slower speeds encourage precipitation), cooling rate, and thermal cycling are also factors influencing TCC [2–4]. It has been shown in previous studies [5,6] that if the  $T_{min}$  drops to below the start of the austenite-to-ferrite transformation,  $Ar_3$ , ferrite forms along the initial austenite grain boundaries where AlN precipitation is accelerated. Nozaki et al. [4] observed that thermal cycling above and below the  $Ar_3$  temperature promotes the formation of proeutectoid ferrite, which intensifies the formation of AlN.

Lekganyane et al. [7] showed that poor ductility in a peritectic C–Mn steel could not be recovered after experiencing a  $T_{min}$  of 730 °C, even when applying a  $T_{max}$  as high

as 1030 °C. This was attributed to the formation of thin ferrite films on the austenite grain boundaries in the  $T_{min}$  temperature region, which remain untransformed during rebounding to temperatures below 930 °C, thereby embrittling the steel. At a  $T_{max}$  of 1030 °C, it was suggested that AlN particles on pre-existing ferrite films at prior austenite grain boundaries, PAGBs, remain undissolved during rebounding and are responsible for the loss in ductility. The current work investigates the mechanism that leads to poor ductility for a  $T_{min}$  of 730 °C by using a combination of microscopy and a precipitation kinetics model applied to the thermal profiles employed in the hot ductility tests.

## 2. Experimental Procedure

**Chemistry:** The chemistry of an as-cast industrial C–Mn slab sample, 240 mm thick, is shown in Table 1. Cylindrical specimens with a diameter of 5 mm and a length of 10 mm were machined from the slab quarter thickness to minimise segregation effects.

**Table 1.** Chemical composition, mass-%. All other elements are residual.

C	Mn	Si	Ni	Cr	P	Al	N	S
0.16	1.03	0.06	0.01	0.02	0.01	0.04	0.0037	0.0030

**Thermal profiles:** Continuous casting simulations were performed on a Bähr dilatometer using the temperature–time profiles employed by Lekganyane et al. [7] in hot ductility tests on a Gleeble 1500D machine. Two  $T_{min}$  temperatures were selected, i.e., 730 and 830 °C, which are 70 °C and 170 °C above the measured  $Ar_{3P}$ , the start of the austenite-to-ferrite transformation temperature during primary cooling. This ensured that the  $T_{min}$  would fall in the single austenite phase; see Table 2. A 10 s isothermal holding period was applied at  $T_{min}$  to homogenise the specimen temperature.  $Ar_{1P}$  is the end of the austenite-to-ferrite transformation temperature during primary cooling, and  $Ar_{3S}$  and  $Ar_{1S}$  are the respective start and end temperatures of the austenite-to-ferrite transformation during secondary cooling. The equilibrium austenite-to-ferrite start transformation temperature,  $Ae_3$ , was calculated from ThermoCalc® [8]

**Table 2.** Measured critical temperatures during primary and secondary cooling [7,8].

Primary Cooling (10 °C/s)		Secondary Cooling (0.1 °C/s)		Equilibrium
$Ar_{3P}$ (°C)	$Ar_{1P}$ (°C)	$Ar_{3S}$ (°C)	$Ar_{1S}$ (°C)	$Ae_3$ (°C)
660	~500	788	640	840

Specimens were heated to 1350 °C at 5 °C/s, soaked for 2 min, primary cooled to a  $T_{min}$  of 730 °C at 10 °C/s, held for 10 s, reheated (rebound) to various  $T_{max}$  values between 780 and 1130 °C, and finally, quenched to room temperature at a rate of 600 °C/s to freeze the microstructure for metallographic studies; see Figure 1. Additional tests included secondary cooling at 0.1 °C/s after rebounding to 1030 °C and quenching from two extreme unbending temperatures,  $T_U$ , i.e., 758 and 958 °C; see Figure 2. The  $T_U$  values were varied between 70 and 270 °C below the  $T_{max}$  to study the influence of undercooling on hot ductility [7]. Specimens were subsequently etched with 2% nital solution to reveal the presence of ferrite at the PAGBs.

**Allotriomorphic ferrite:** The amount of ferrite present in the PAGBs was quantified using Image J® software. Twelve sites were measured per specimen using the linear-intercept method. Gridlines of known length were placed on a micrograph and the number of ferrite allotriomorphs intercepting the lines in the horizontal and vertical axes were counted per unit length. All Widmanstätten ferrite was ignored, as it would have formed during the quench.

**AlN precipitation:** TC-PRISMA, together with the TCFE12 and MOFE7 steel databases [9], were employed to predict the grain boundary precipitation kinetics of AlN in either ferrite

(bcc) or austenite (fcc) for the thermal profiles in Figures 1 and 2. Elemental segregation was not considered, and the total Al and N contents were used to conservatively monitor the progress of precipitation.

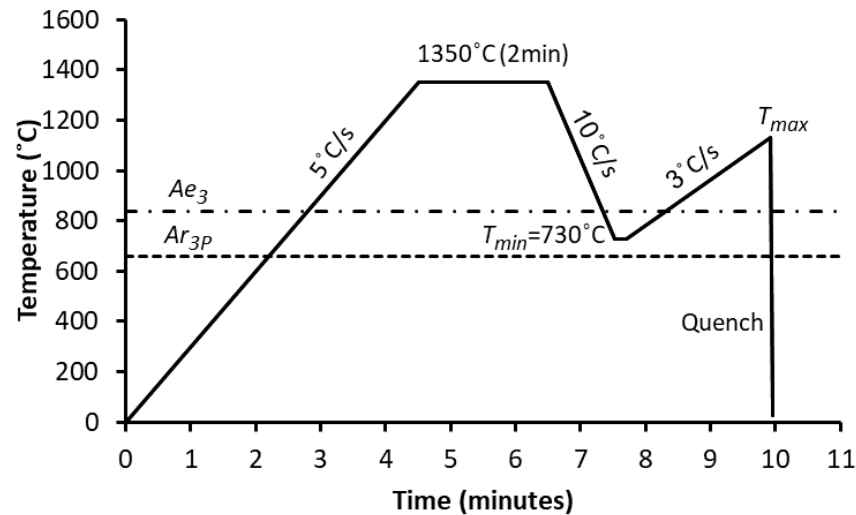


**Figure 1.** Thermal profiles used for evaluating the presence of ferrite during rebounding from  $T_{min} = 730\text{ }^{\circ}\text{C}$  to various  $T_{max}$  values ( $780\text{--}1130\text{ }^{\circ}\text{C}$ ).  $Ae_3 = 840\text{ }^{\circ}\text{C}$  and  $Ar_{3p} = 660\text{ }^{\circ}\text{C}$ .

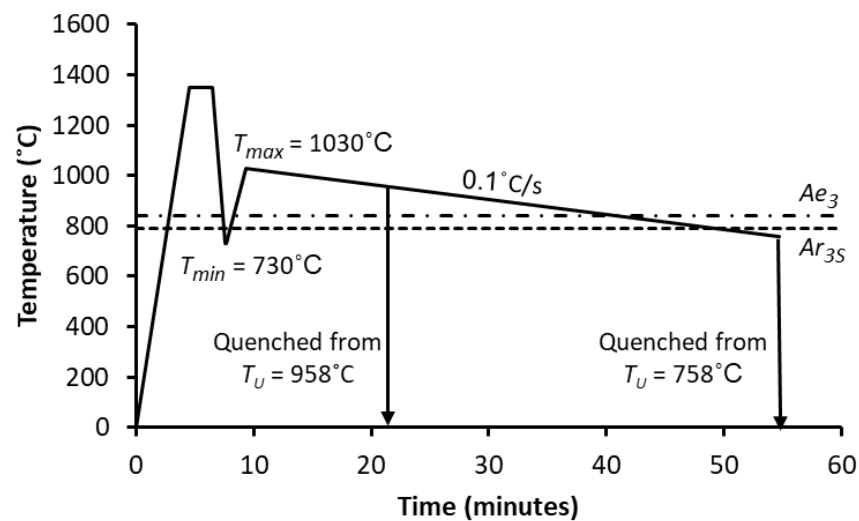
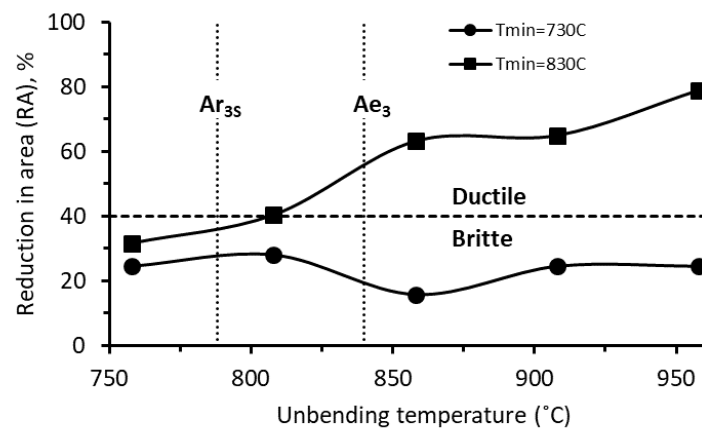


**Figure 2.** Thermal profiles used to evaluate the presence of thin ferrite films at the unbending temperature before unbending  $T_{min} = 730\text{ }^{\circ}\text{C}$ .  $Ae_3 = 840\text{ }^{\circ}\text{C}$  and  $Ar_{3s} = 788\text{ }^{\circ}\text{C}$ .

### 3. Results

#### 3.1. Hot Ductility

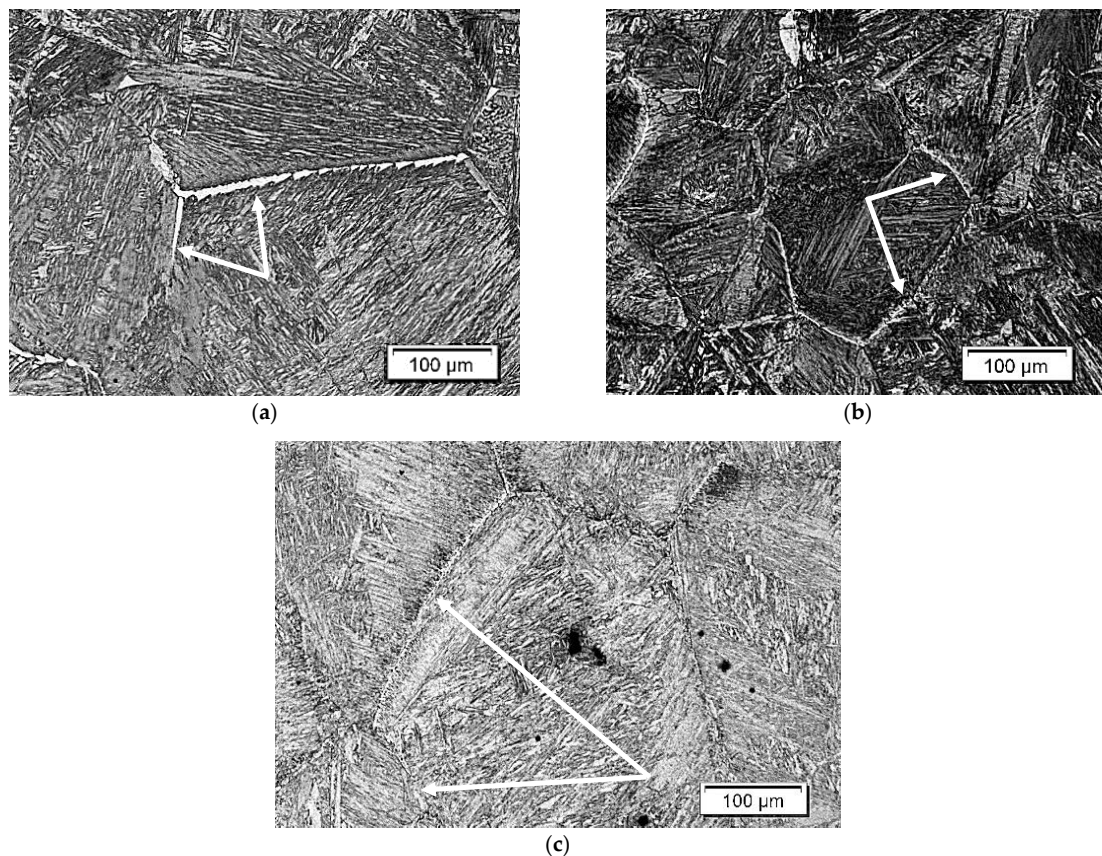
An RA of 40% is considered to be the minimum ductility required to avoid transverse cracking during continuous casting [10]. Figure 3 shows that for a  $T_{max}$  of  $1030\text{ }^{\circ}\text{C}$ , primary cooling to a  $T_{min}$  of  $730\text{ }^{\circ}\text{C}$  produced poor ductility [7], i.e., low reduction-in-area (RA) values at all unbending temperatures, whereas a  $T_{min}$  of  $830\text{ }^{\circ}\text{C}$  produced superior ductility, which improved with rising  $T_U$  values. Metallographic examination of the fracture surfaces showed that for a  $T_{min}$  of  $730\text{ }^{\circ}\text{C}$ , brittle intergranular failure occurred at all  $T_U$  temperatures, whereas ductile fracture was found after a  $T_{min}$  of  $830\text{ }^{\circ}\text{C}$  [7]. Similar results were found for specimens that were in situ melted ( $T > 1400\text{ }^{\circ}\text{C}$ ) in an attempt to generate an as-cast initial microstructure [8].



**Figure 3.** Influence of  $T_{min}$  on hot ductility for  $T_{max} = 1030$  °C. Poor ductility resulted at all unbending temperatures after a  $T_{min}$  of 730 °C [7].  $Ae_3 = 840$  °C and  $Ar_{3P} = 660$  °C.

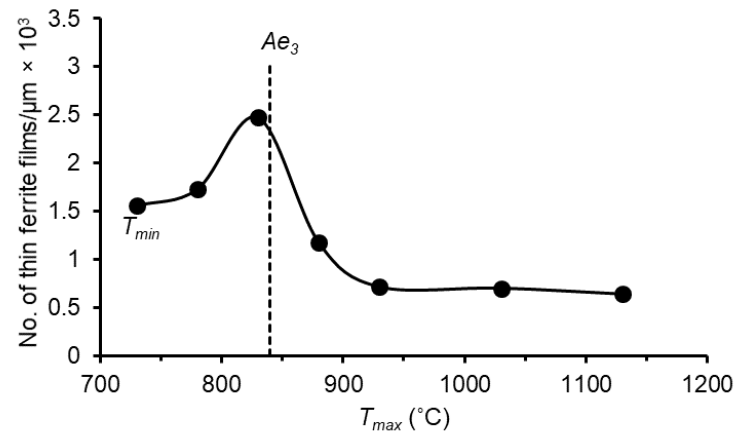
### 3.2. Quenched Microstructures after Primary Cooling

Figure 4 shows the presence of PAGB thin ferrite films in the quenched microstructure from a  $T_{min}$  of 730 °C up to a rebound of 1130 °C. The thickness of the ferrite films decreases with increasing  $T_{max}$ . This result contrasted with dilatometry plots that indicated an apparent fully austenitic microstructure at and above 930 °C [7]. In Figure 5, the amount of ferrite increases from  $T_{min}$ , peaks at a  $T_{max}$  of 830 °C, and then decreases with an increase in rebound temperature, eventually reaching a trough at 930 °C. This indicates that the ferrite transformation back to austenite is sluggish. No thin films were observed after quenching from any  $T_{max}$  after a  $T_{min}$  of 830 °C [7].



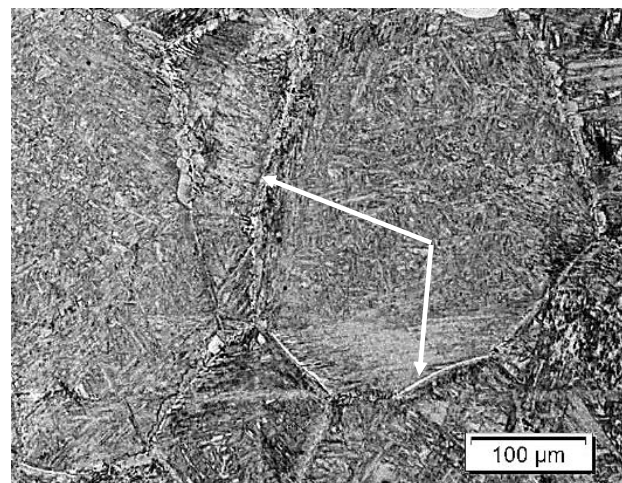
**Figure 4.** Microstructures of specimens quenched from (a)  $T_{min} = 730$  °C before rebounding, and from a  $T_{max}$  of (b) 830 °C and (c) 1130 °C. The thin ferrite films (arrows) get thinner with increasing  $T_{max}$ .



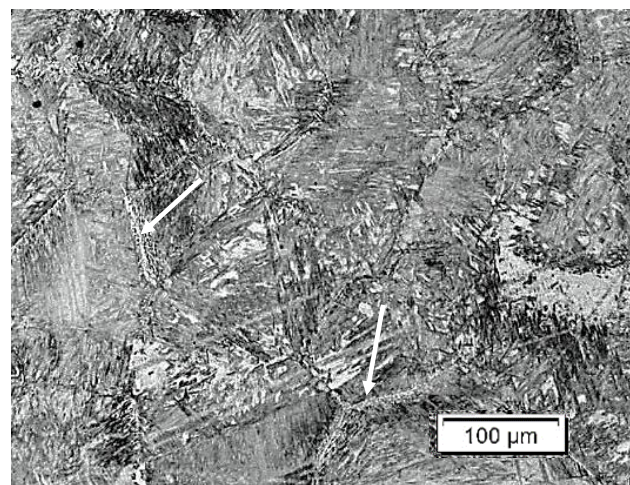


**Figure 5.** PAGBs thin ferrite film concentration as a function of rebound temperature ( $T_{max}$ ) from a  $T_{min}$  of 730 °C. After an initial increase below  $A_{e3}$ , the number of films drops sharply above 830 °C due to re-austenitisation but stabilizes at approximately 930 °C.

Ferrite that forms during the rebound remains on the PAGBs during secondary cooling up to  $T_U$ ; see Figure 6. As expected, more PAGB thin ferrite films were found at the lower  $T_U$  of 758 °C, which is below both  $A_{e3}$  and  $A_{r35}$ .



(a)



(b)

**Figure 6.** Quenched microstructures from a  $T_U$  of (a) 758 °C and (b) 958 °C before deformation, showing the presence of thin ferrite films on PAGBs (arrows).

### 3.3. Precipitation of AlN in Ferrite and Austenite

Figure 7 shows that for a  $T_{min}$  of 730 °C, the predicted volume fraction of AlN in ferrite (bcc) increases exponentially with rebound temperature from 900 °C after 60 s (125 s total time) from  $T_{min}$ , peaking at 1070 °C, only to rapidly decrease again at higher temperatures and dissolve completely at 1200 °C. There is virtually no predicted AlN formation when  $T_{min}$  is restricted to 830 °C, consistent with the absence of thin ferrite films found earlier [7]. Figure 8 shows that the predicted AlN precipitation begins at 930 °C where the ferrite content starts to form a fairly constant, low volume base. Aluminium concentrations due to segregation at grain boundaries are expected to start precipitation earlier and extend it to even higher temperatures than those shown. The solute Al content remains high at all  $T_{max}$  and may have a stabilizing effect on the ferrite films during both the rebound and secondary cooling.

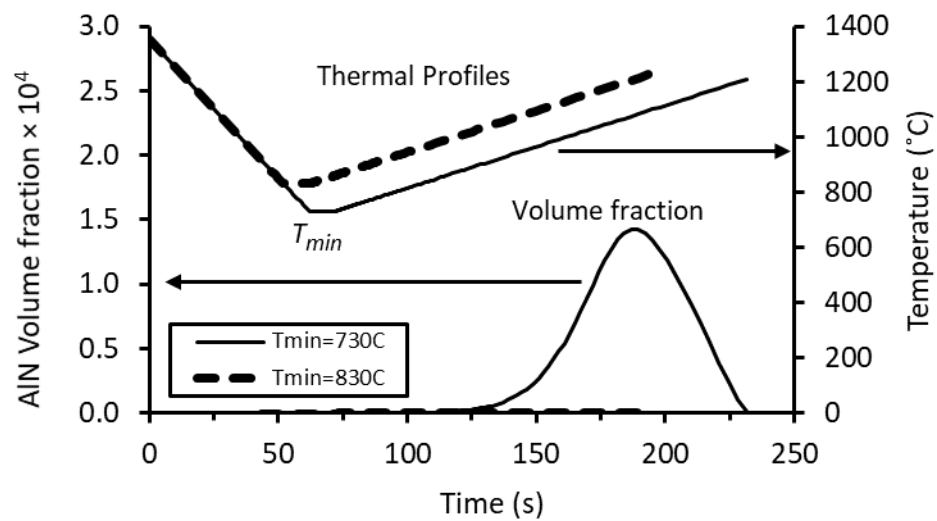


Figure 7. Volume fraction of AlN in ferrite (bcc) predicted by TC-PRISMA [9] as a function of  $T_{min}$  thermal profile (time-temperature) to a rebound temperature above 1200 °C.

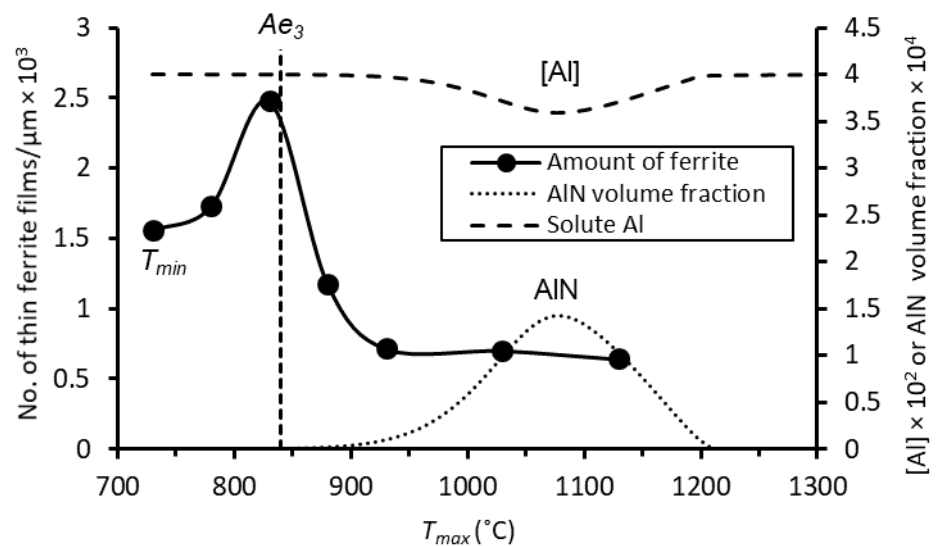
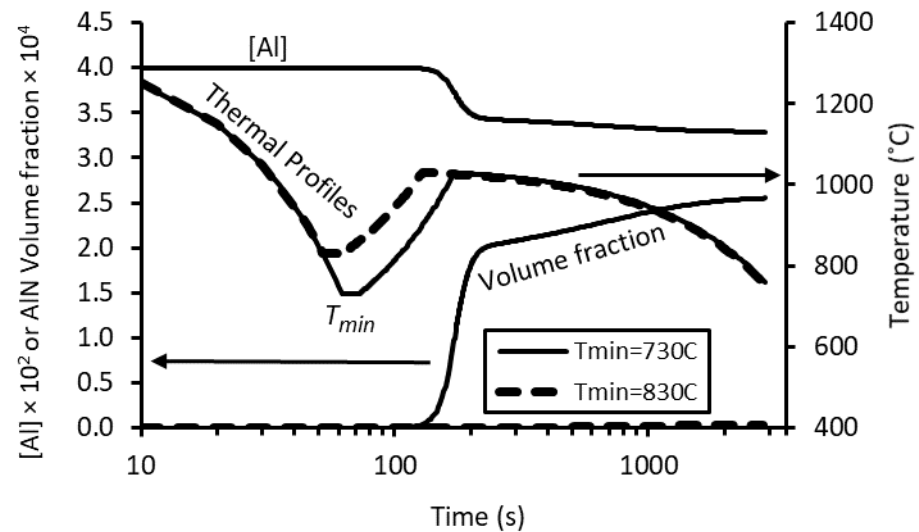


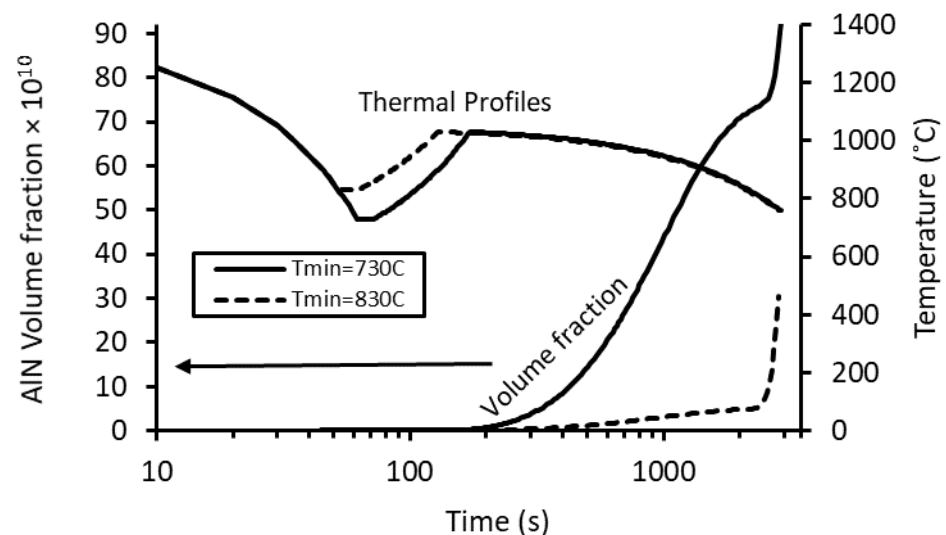
Figure 8. Amount thin ferrite films, predicted AlN volume fraction (TC-PRISMA) and total solute Al as a function of  $T_{max}$  from a  $T_{min}$  of 730 °C.

Figure 9 plots the evolution of AlN volume fraction and solute Al along the entire thermal profile at the slab corner surface used for hot ductility testing. For a  $T_{min}$  of 730 °C and corresponding  $T_{max}$  of 1030 °C, the AlN volume fraction increases sharply up to the

$T_{max}$  and then slowly increases during the secondary cooling until it reaches the minimum  $T_U$  of 758 °C. Only about 18% of the total Al forms AlN; the balance remains in solution until the unbending temperature is reached. No AlN was predicted to form at any stage of the process for a  $T_{min}$  of 830 °C. No significant AlN formation in austenite (fcc) was predicted [9] (see Figure 10) when following the same thermal profile as that in Figure 9 for all  $T_{min}$ . The calculated mean AlN particle radius increases with time up to 100 nm at the lowest unbending temperature of 758 °C (see Figure 11) and follows the volume fraction curve.



**Figure 9.** AlN volume fraction in ferrite (bcc) and total solute Al predicted by TC-PRISMA [9] as a function of  $T_{min}$  thermal profile (temperature-time) to a rebound temperature of 1030 °C and during subsequent secondary cooling.



**Figure 10.** Extremely low AlN volume fraction in austenite (fcc) predicted by TC-PRISMA [9] as a function of  $T_{min}$  and rebound temperature of 1030 °C.

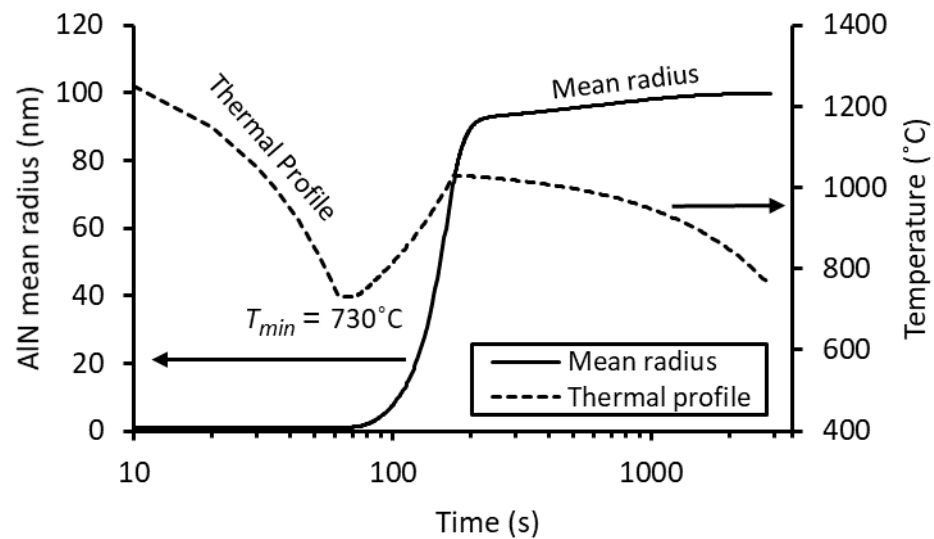


**Figure 11.** Mean AlN particle radius in ferrite (bcc) predicted by TC-PRISMA [9] for a  $T_{min}$  of 730 °C thermal profile to a rebound temperature of 1030 °C and during subsequent secondary cooling.

#### 4. Discussion

##### 4.1. Hot Ductility

The influence of  $T_{min}$  and  $T_U$  on ferrite film formation and predicted AlN evolution were examined under constant heating, cooling and strain rates conditions in continuous casting.

$T_{min} = 730$  °C: The poor hot ductility at all  $T_U$  values in Figure 3 is attributed, in part, to the presence of ferrite films on the PAGBs that formed during rebounding between  $T_{min}$ , and  $T_{max}$  temperatures. Although most of the ferrite transforms back to austenite during this stage, a small untransformed fraction remains above 930 °C up to  $T_U$ ; see Figures 4–6. TC-PRISMA predicts [9] that the primary cooling rate of 10 °C/s is sufficiently fast to completely retard nucleation of AlN, a precipitate known to be detrimental to hot ductility. After subjecting the slab corner surface to a sufficiently low  $T_{min}$ , 730 °C in this case, AlN forms in bcc ferrite during the rebound and continues to precipitate and grow during secondary cooling; see Figures 9 and 11. Nozaki et al. [4] also showed that the formation of AlN is accelerated in C–Mn slabs when rebounding is applied from a low temperature up to and above 700 °C.

The combined presence of thin ferrite films and AlN on PAGBs during unbending is thought to be responsible for the poor ductility at all test temperatures. The small amount of ferrite on PAGBs weakens them since ferrite is softer than austenite at a given temperature. This leads to high localised strain concentration and voiding around inclusions and particles eventual cracking. The presence of particles, such as AlN with sufficiently large volume fractions and small interparticle spacings promote austenite grain boundary sliding leading to cracking at the PAGBs [10]. The brittle intergranular failure shown in earlier work [7] is testament to the presence of AlN and thin films at the PAGBs. Mintz et al. [2] have shown that poor ductility is always associated with intergranular failure at the austenite grain boundaries. TC-PRISMA predictions of AlN precipitation kinetics are expected to be significantly enhanced if conservative total elemental contents are replaced in calculations by Al and N concentrations at grain boundaries as a result of segregation during solidification.

$T_{min} = 830$  °C: Thin ferrite films do not form after a  $T_{min}$  of 830 °C [7]. This reduces the driving force for AlN formation on the PAGBs and results in good ductility due to the absence of grain boundary embrittlement being experienced during unbending. Further, the absence of intergranular failure after metallographical examination on the fracture surfaces above a  $T_U$  of 850 °C [7] strongly suggests that no particles or ferrite films formed at the austenite grain boundaries during primary cooling, rebounding or secondary cooling.



The lower ductility experienced at a  $T_U$  of 810 °C which is below the  $Ae_3$  is due to the formation of strain-induced ferrite during the unbending process [10]. Unbending even lower at a  $T_U$  of 760 °C which is below  $Ar_{3S}$  promotes formation of ferrite thin films during slow continuous secondary cooling.

For both  $T_{min}$ , ductility was recovered when unbending temperatures were below 700 °C due to a high-volume fraction of ferrite [7,8].

#### 4.2. Formation of Ferrite above $Ar_{3P}$

Firstly, the formation of ferrite above the  $Ar_{3P}$  during primary cooling can be attributed to the 10 s isothermal hold for stabilisation as well as the time exposed to the ferrite transformation nose upon reheating, both promoting the formation of ferrite. A TTT diagram for a similar chemistry (0.17% C–0.92% Mn) [11] austenitised at 1316 °C shows that a 10 s hold at 730 °C exceeds the ferrite nose start time. Secondly, the formation of ferrite above the  $Ar_{3P}$  may be due to the high undercooling ( $Ae_3-T_{min}$ ) of 110 °C for a  $T_{min}$  of 730 °C compared to the small undercooling of 10 °C for a  $T_{min}$  of 830 °C. The high undercooling at 730 °C promotes ferrite formation during cooling and subsequently during reheating below the  $Ae_3$  due to the increased driving force for nucleation. This was confirmed by dilation curves [7] and the microstructures in Figure 4, where the amount of thin ferrite films at the PAGBs (see Figure 5) initially increased from  $T_{min} = 730$  to a  $T_{max}$  of 830 °C and subsequently decreased above  $Ae_3$  due to re-austenitisation.

#### 4.3. Metallography vs. Dilatometry

Dilatometry indicated that the transformation of ferrite (films) back to austenite should be complete above 930 °C [7], which is clearly not the case, as it was shown metallographically to be present after rebound temperatures up to 1130 °C; see Figure 4. This discrepancy is attributed to the extremely small volume fraction of thin ferrite films above 930 °C, which was undetectable by dilatometry and resulted in an essentially linear thermal expansion.

#### 4.4. Ferrite Decomposition during Rebounding

The existence of thin ferrite films at temperatures as high as 1130 °C, albeit in small amounts, cannot be readily explained without further work. A recent study showed the existence of ferrite as high as 1350 °C due to dynamic transformation in C–Mn steels [12]. However, in the current work, the only applied strain is during unbending i.e., no deformation occurs between  $T_{min}$  and  $T_{max}$ .

The observed presence of ferrite films at temperatures well above 930 °C corresponds with TC-PRISMA prediction [9] of AlN precipitation occurring in bcc ferrite at these high temperatures, as opposed to the almost complete absence of AlN in fcc austenite under the same conditions; see Figures 9 and 10. AlN precipitation is very slow in austenite, but it forms rapidly in ferrite [13]. TC-PRISMA indicates high Al solute contents at all  $T_{max}$  and that an AlN precipitation peak falls within the temperature region above 930 °C, where ferrite forms a low volume base; see Figure 8. The delay in the ferrite decomposition during rebounding may be attributed primarily to the strong ferrite stabilising effect of Al, and secondly, to the precipitation of AlN.  $T_{max}$  values above 1130 °C were outside the scope of the current work and were not studied metallographically. It is expected that if indeed AlN is responsible for delaying the ferrite decomposition, the volume fraction of thin ferrite films will decrease significantly above 1130 °C and completely transform at 1200 °C. Further work is required to explain the exact mechanism of how AlN delays the decomposition of ferrite.

#### 4.5. Relevance to Advanced High Strength Steels (AHSS)

Although the current study was carried out on plain C–Mn steel, it is expected that the above findings should be applicable to all grades where poor ductility is associated with thin ferrite films and AlN particles on the PAGBs, especially TWIP and TRIP steels that contain high concentrations of Al (1–5%). Further work is required to confirm this.

## 5. Conclusions

1. The poor observed ductility in C–Mn steel at all practical unbending temperatures following a minimum primary cooling temperature of 730 °C is due to austenite grain boundary embrittlement as a result of thin ferrite film formation, which persists during rebounding to all tested temperatures and promotes the formation of detrimental AlN precipitation.
2. The superior hot ductility following primary cooling to 830 °C, as opposed to a  $T_{min}$  of 730 °C, is attributed to the absence of both thin ferrite films and AlN precipitation, as predicted by TC-PRISMA.

**Author Contributions:** Conceptualization, D.R.N.M., R.J.M. and K.M.B.; investigation, D.R.N.M.; writing—original draft preparation, D.R.N.M., R.J.M. and K.M.B.; writing—review and editing, R.J.M. and K.M.B. All authors have read and agreed to the published version of the manuscript.

**Funding:** This research received no external funding.

**Data Availability Statement:** Data presented in this article is available at request from the corresponding author.

**Acknowledgments:** Thanks to V. Kurup for assistance with the Thermo-Calc® (TC-PRISMA) software and to T. Sithole & F. Magwala for metallography ferrite volume fraction measurements.

**Conflicts of Interest:** The authors declare no conflict of interest.

## References

1. Schrewe, H.F. Strand mechanics, bending, straightening and bulging. In *Continuous Casting of Steel: Fundamental Principles and Practice*; Verlag Stahleisen: Düsseldorf, Germany, 1987; pp. 138–144, ISBN 3-514-00389-0.
2. Mintz, B.; Yue, S.; Jonas, J.J. Hot ductility of steels and its relationship to the problem of transverse cracking during continuous casting. *Int. Mater. Rev.* **1991**, *36*, 187–220. [[CrossRef](#)]
3. Abushosha, R.; Ayyad, S.; Mintz, B. Influence of cooling rate on hot ductility of C-Mn-Al and C-Mn-Nb-Al steels. *Mater. Sci. Technol.* **1998**, *14*, 346–351. [[CrossRef](#)]
4. Nozaki, T.; Matsuno, J.; Murata, K.; Ooi, H.; Kodama, M. A secondary cooling pattern for preventing surface cracks on continuous casting slab. *Trans. ISIJ* **1978**, *18*, 330–338. [[CrossRef](#)]
5. Coleman, T.H.; Wilcox, J.R. Transverse cracking in continuously cast HSLA slabs—influence of composition. *Mater. Sci. Technol.* **1985**, *1*, 80–83. [[CrossRef](#)]
6. Suzuki, K.; Miyagawa, S.; Saito, Y.; Shiotani, K. Effect of microalloyed nitride forming elements on precipitation of carbonitride and high temperature ductility of continuously cast low carbon Nb containing steel slab. *ISIJ Int.* **1995**, *35*, 34–41. [[CrossRef](#)]
7. Lekganyane, K.M.; Mostert, R.J.; Siyasiya, C.W.; Banks, K.M. Irreversible loss of hot ductility following simulated primary cooling of a C–Mn steel to temperatures above the ferrite transformation temperature. *Mater. Sci. Eng. A* **2021**, *810*, 141007. [[CrossRef](#)]
8. Lekganyane, K.M. Influence of primary cooling conditions and austenite conditioning on the hot ductility of simulated continuous cast peritectic steels. Master’s Thesis, Dept. of Materials Science and Metallurgical Engineering, University of Pretoria, Pretoria, South Africa, 2020.
9. Andersson, J.O.; Helander, T.; Höglund, L.; Shi, P.F.; Sundman, B. Thermo-Calc version 2022b and DICTRA, Computational tools for materials science. *Calphad* **2002**, *26*, 273–312. [[CrossRef](#)]
10. Mintz, B. The Influence of Composition on the Hot Ductility of Steels and to the Problem of Transverse Cracking. *ISIJ Int.* **1999**, *39*, 833–855. [[CrossRef](#)]
11. Vander Voot, G.F. *Atlas of Time-Temperature Diagrams for Irons and Steels*; ASM International: Reading, PA, USA, 1991; p. 13, ISBN 0-87170-415-3.
12. Aranas, C., Jr.; Grewal, R.; Chadha, K.; Shahriari, D.; Jahazi, M.; Jonas, J.J. Formation of widmanstätten ferrite in a C-Mn steel at temperatures high in the austenite phase field. In Proceedings of the International Conference on Solid-Solid Phase Transformations in Inorganic Materials (PTM 2015), Whistler, BC, Canada, 28 June–3 July 2015; pp. 613–620.
13. Wilson, F.G.; Gladman, T. Aluminium nitride in steel. *Int. Mater. Rev.* **1988**, *33*, 221–287. [[CrossRef](#)]